ELSEVIER

Journal of Volcanology and Geothermal Research 102 (2000) 319–338

Journal of volcanology and geothermal research

www.elsevier.nl/locate/jvolgeores

Magmatic history of the East Rift Zone of Kilauea Volcano, Hawaii based on drill core from SOH 1

S.L. Quane[1,a], M.O. Garcia[a,*], H. Guillou[b], T.P. Hulsebosch[†,a]

[a]*Department of Geology and Geophysics, Hawaii Center for Volcanology, University of Hawaii, Honolulu, HI 96822, USA*
[b]*Laboratoire des Sciences du Climat et de l'Environnement, Domaine du CNRS, 91198 Gif-Sur-Yvette, France*

Received 22 November 1999; received in revised form 3 March 2000; accepted 3 March 2000

Abstract

Deep drilling has allowed for the first time an examination of most of the shield stage of a Hawaiian volcano when it is centered over the hotspot and most of its volume is produced. We determined the lithologies, ages, geochemical characteristics and accumulation rates of rocks from the continuously cored, ~1.7 km deep Scientific Observation Hole (SOH) 1, which was drilled into Kilauea's East Rift Zone. The uppermost ~750 m of this hole contain relatively unaltered subaerially quenched lavas; the lower portion is a mixture of weakly to moderately altered hyaloclastites and massive basalts intruded by dikes. Unspiked K–Ar dating was attempted on 14 lavas but only four yielded geologically reasonable ages. The oldest age is 351 ± 12 ka for a sample from 1541 m. Eighty XRF major and trace element analyses of lavas from throughout the section demonstrate that these lavas have the same compositional range as historical Kilauea lavas and that there was no systematic geochemical variation for the volcano over the last 350 ka. Kilauea's average yearly magma supply during this period was probably ~ 0.05 ± .01 km^3, which is identical to its average historical magma supply rate. Thus, Kilauea's overall source and melting conditions have remained remarkably constant for the last 350 ka despite its having drifted ~42 km over the Hawaiian plume. These results require that the portion of the plume being melted to produce Kilauea magmas be relatively large and well mixed, which is inconsistent with models that place this source on the margin of a radially zoned plume.

Keywords: Kilauea volcano; Drill core; K–Ar geochronology; Geochemistry; Mantle plumes

1. Introduction

Mantle plumes provide an important means of transferring heat and mass from the deep mantle to the crust (e.g. Sleep, 1990). Models for the structure of mantle plumes depend on reconstructing the magmatic history of the volcanoes they produce (e.g. DePaolo and Stolper, 1996). The Hawaiian Islands are the classic example of plume-generated volcanoes but their frequent eruptions and rapid subsidence greatly limit attempts to reconstruct the magmatic history of individual volcanoes. Thus, it has been necessary to manufacture a 'composite' Hawaiian volcano using outcrops from many volcanoes (e.g. Macdonald et al., 1983). Such reconstructions are inherently flawed. They have substantial age gaps, especially for the shield stage of volcanism. Also, they assume that the composition of the plume

* Tel.: + 1-808-956-6641; fax: + 1-808-956-3188.
E-mail addresses: squane@eos.ubc.ca (S.L. Quane), garcia@soest.hawaii.edu (M.O. Garcia).
[1] Present address: Department of Earth and Ocean Sciences, University of British Columbia, Vancouver, BC, Canada V6T 1Z4.
[†] Deceased.

0377-0273/00/$ - see front matter
PII: S0377-0273(00)00194-3

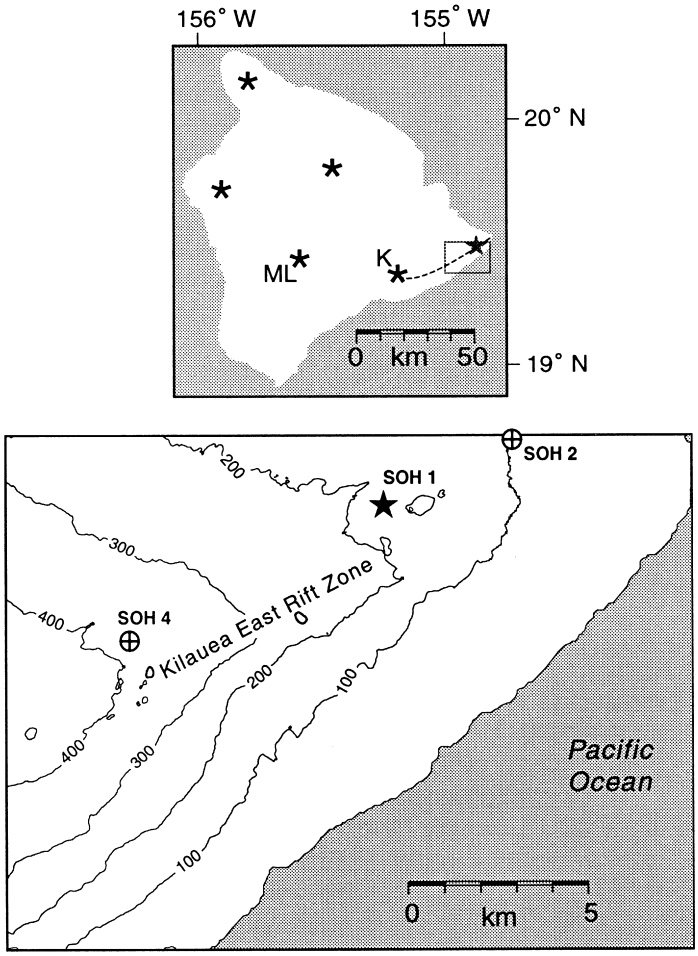

Fig. 1. Location map for the Scientific Observation Holes along Kilauea's lower east rift zone. The location of SOH 1 is shown by a star; SOH 4 and SOH 2 are shown by ⊕. The three holes form a straight line along the crest of the KERZ. Contour interval is 100 m and the gray area is the Pacific Ocean. The inset map shows the location of SOH 1 (star) on the island of Hawaii, the summits (marked by ∗) of the island's five shield volcanoes (K: Kilauea; ML: Mauna Loa), and the location of Kilauea's east rift zone (dashed line).

and its melting processes have been relatively constant over at least a few million years. There is ample evidence that even adjacent Hawaiian shield volcanoes have significant differences in their extent of partial melting and source composition (e.g. Kilauea vs. Mauna Loa volcanoes; Kurz et al., 1995; Pietruszka and Garcia, 1999). Thus, it is essential that the long-term history of an individual Hawaiian volcano be examined if we are to realistically evaluate the structure and melting history of mantle plumes. Deep drilling is the only viable method for achieving this goal.

Three Scientific Observation Holes (SOH 1, SOH 2, and SOH 4) were drilled into lower Kilauea's East Rift Zone (KERZ; Fig. 1) between 1989 and 1991 to assess its geothermal resources. The cores from these 1.7–2.0 km deep holes sample a major segment of Kilauea's history, and were thought to have the potential to penetrate into Kilauea's pre-shield stage and/or the underlying older Mauna Loa basalts. This study examined rock cores from the 1685 m deep SOH 1 because it was continuously cored with a high core recovery (~95%) and its rocks are relatively unaltered. Although SOH 4 was continuously cored to a greater depth (2001 m), temperatures were 100–150°C higher at a given depth and secondary minerals

are more common in its lavas than those from SOH 1 (Bargar et al., 1995). Only the lower portion of SOH 2 was cored, so it was not considered for this time-series analysis.

Kilauea Volcano is one of the most active and intensely studied volcanoes on Earth, yet its prehistoric record is not well documented (Tilling and Dvorak, 1993). Ninety percent of its surface exposures are younger than 1.5 ka (Holcomb, 1987), its thickest exposure is only ~300 m, and no surface lava is older than ~100 ka (caution: this age is based on lava accumulation rate estimates, not on geochronology; Easton, 1987). A geochemical study of these older surface lavas (the Hilina Basalts, >25 ka; Easton, 1987) found that their compositions to be identical to historical Kilauea lavas, which are distinct from those of the adjacent, historically active Mauna Loa Volcano (Chen et al., 1996). The overall age of Kilauea has been estimated using lava accumulation rates at ~150 ka (Lipman, 1995) to 200–300 ka (Easton, 1978).

This study presents a summary of the lithology, age, petrography, and geochemistry of the SOH 1 drill core. Fourteen lavas were selected for unspiked K–Ar geochronology and 80 rocks were analyzed by XRF for major and trace elements. The new ages demonstrate that the volcano is much older than previous field-based estimates and that it has been in its shield building stage for at least 350 ka. During this period, the compositional range of Kilauea lavas remained unchanged. Likewise, long-term magma supply rates for this period are identical to the average historical rate. These results require long-term stability in melting processes and a large (>42 km across), well-mixed source within the Hawaiian plume for Kilauea magmas. Thus, it is unlikely that the source of Kilauea magmas is located on the margin of a radially zoned plume, as previously suggested.

2. Core lithology

The SOH 1 core was subdivided into lithologic units based on a visual examination. Baked, rubbly, and/or glassy contacts and abrupt changes in mineralogy were used to identify unit contacts. The lithologic units include a'a and pahoehoe flows, massive basalts, dikes, hyaloclastites, lithified breccia, loose rubble, sand, and ash. Flows with rubbly tops and bottoms and sheared vesicles were identified as a'a. Flows with smooth or ropy glassy contacts and abundant round vesicles were identified as pahoehoe. Units with glassy or high-angle glassy contacts, very little to no vesicularity, and less alteration than adjacent rocks were identified as dikes. Fragmental rocks are common in the lower half of the core. Most are hyaloclastites consisting of weakly to moderately indurated, poorly sorted, vesicular, glassy clasts <1–5 cm in diameter. Many of the hyaloclastites contain lava fragments up to 1 m long, with the same mineralogy and vesicularity as the smaller clasts. Thicker lava intervals (>2 m) within the hyaloclastite section are called massive basalts because their flow types could not be identified. Fragmental units with non-vesicular clasts are termed dike breccias. One unit with coral reef and lava flow fragments in a carbonate-bearing matrix was classified as a carbonate breccia.

The ~1.7 km of core from SOH 1 was subdivided into 368 lithologic units. The most common unit type is lava flows (62.2%) with 36.4% a'a, 22.0% pahoehoe and 3.8% massive basalt. Dikes comprise 26.7% of the units, hyaloclastites 7.6%, breccias 2.1%, and subaerial fragmental debris ~1.4% (Fig. 2). This perspective changes somewhat if the rock type is evaluated relative to its volumetric abundance in the section. Lava flows are less abundant (45.1%) with a'a dominating other flow types (30.7% vs. 9.8% for pahoehoe, and 4.6% massive basalt) and dikes are more abundant (36.4%). Hyaloclastite represents 13.2% of the section and breccia (and other debris) account for 5.3%. The upper 740 m of the hole are almost entirely subaerially quenched lava flows and the section below 1200 m is mostly dikes (Fig. 2). The thickness of a'a flows ranges from <1–12 m; pahoehoe flows are <1–5 m thick. There is no systematic change in flow thickness within the subaerial flow section. The dominance of a'a flows within the core is surprising because only 16% of Kilauea's surface is covered by a'a (Holcomb, 1987) and the hole is located along the axis of the east rift zone (Fig. 1) where pahoehoe lava is more common. However, a'a flows are more prevalent along the lower portion of the east rift zone than elsewhere on Kilauea (Holcomb, 1987), which is thought to be related to the more differentiated composition (and cooler

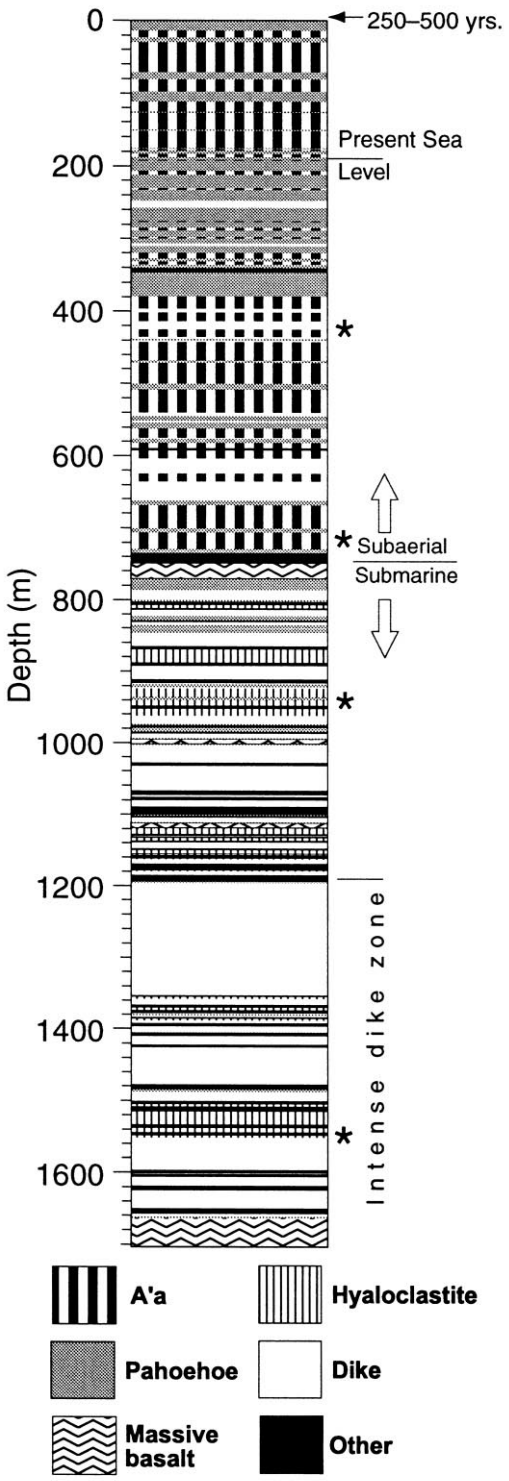

temperature during eruption) of these lavas (<6.8 wt.% MgO; Moore, 1983).

A carbonate breccia at ~740 m depth marks the boundary between exclusively subaerial units to interbedded subaerial and submarine units below. The submarine section consists of interfingering hyaloclastites and massive basalts (including pillow basalt fragments). No coherent pillow lava flow units were identified. Dikes are sparse above the submarine-subaerial transition and increase in abundance down-section; they dominate below ~1200 m. The samples in this study are numbered according to their depth of recovery in meters within the hole.

3. Geochronology

Dating young (<1 Ma), low potassium (<1 wt.%) rocks is inherently difficult using either conventional K–Ar or Ar–Ar techniques. The unspiked K–Ar technique (also known as the Cassignol method) was employed for this study because it has proven effective in dating very young (<100 ka) Hawaiian volcanic rocks (Guillou et al., 1997a,b). This method precisely measures minor variations in the $^{40}Ar/^{36}Ar$ ratio between a standard and unknown. In order to optimize success in dating SOH 1 lavas, strict guidelines were used to select only unaltered lava flows. These flows have low vesicularity (<10%), holocrystalline groundmass, and K_2O/P_2O_5 between 1.3 and 2.0 (unaltered Kilauea tholeiitic basalts have ratios of 1.5–2.0; Wright, 1971). Sample preparation procedures are the same as those described by Guillou et al. (1997a). K and Ar measurements were performed on groundmass aliquots. K was analyzed by atomic and flame emission spectrophotometry. Ar was released from the sample by radio frequency induction heating and measured using mass spectrometry. For more details on the unspiked K–Ar technique, see

Fig. 2. Stratigraphic section showing rock type variation for the SOH 1 core. Rock type determinations are based on methods described in the text. The subaerial–submarine contact is ~740 m depth; the zone of greatest dike intensity is from 1200 to 1650 m in the hole. The asterisks show the location of the samples that yielded positive radiometric ages. The age of the uppermost flow in this section has been inferred based on geologic mapping and C^{14} dating (Holcomb, 1987).

Table 1
K–Ar ages of samples from SOH 1. Age calculations are based on the decay and abundance constants from Steiger and Jäger (1977)

Depth (m)	K (wt.%)	Weight molten (g)	^{40}Ar (%)	^{40}Ar (10^{-13} mol/g)	Age ($\pm 2\sigma$) (ka)	Age mean value
Samples giving positive ages						
1550.5	0.168 ± 0.002	1.63820	0.209	1.0439	358 ± 11	
		1.34709	0.221	1.0007	343 ± 22	351 ± 12
940.5	0.279 ± 0.003	1.55585	0.435	0.9306	192 ± 18	
		1.52914	0.394	0.7569	156 ± 24	174 ± 15
755.9	0.493 ± 0.005	1.52053	0.137	0.2486	29 ± 9	
		1.96710	0.103	0.2262	26 ± 9	28 ± 6
409.0	0.394 ± 0.004	2.03647	0.022	0.034	5 ± 5	5 ± 5
		2.03647	−0.008	<0		
Samples giving zero ages						
234.4	0.427 ± 0.010	0.90382	−0.158	<0		
537.4	0.547 ± 0.005	1.58540	−0.034	<0		
691.9	0.502 ± 0.009	1.56385	0.010	0.0249	3 ± 30	

Cassignol and Gillot (1982) and Gillot and Cornette (1986).

Fourteen samples from throughout SOH 1 were selected for unspiked K–Ar geochronology. Eleven of the fourteen samples are from above the submarine–subaerial transition. This sampling bias is due to the scarcity of suitable lavas below the submarine–subaerial transition that meet the selection criteria. Despite the stringent sample criteria, only four of the samples gave geologically meaningful ages (Table 1). No radiogenic argon was measured in 10 of the samples (Table 1). The lack of radiogenic argon in sample 624.8 could be explained by its location between two dikes, which may have caused heating of the rock and ^{40}Ar loss. The lack of radiogenic argon in the other samples demonstrates the inherent difficulties in dating young rocks with low amounts of K (<0.5 wt.%) and ^{40}Ar ($\ll 1\%$). Three of the ages were successfully replicated and these samples cover much of the SOH 1 hole (Table 1). The date for shallowest samples was not duplicated and must be considered only an approximate age. The age of the surface flow at the SOH 1 location is estimated to be 250–500 years old based on geologic mapping and C^{14} ages (Holcomb, 1987).

4. Petrography

In hand specimen, most SOH 1 rocks appear to be aphyric to weakly olivine and plagioclase phyric. Eighty thin sections were examined to better characterize the petrography and degree of alteration of the SOH 1 core. Fifty-one sections are from subaerial (65% a'a and 35% pahoehoe) and submarine lava

Table 2
Vesicle-free modal mineralogy of phenocrysts (>0.5 mm), vesicle percentages and whole-rock MgO content for selected SOH 1 lavas. Modes based on 400 points counted/sample and are in vol%. Cpx—clinopyroxene; Plag—plagioclase

Depth (m)	Olivine	Cpx	Plag	Matrix	Vesicles	MgO (wt%)
14.0	0.1	2.0	1.0	96.9	20	6.6
57.3	3.0	3.0	0.1	93.9	6	10.1
165.5	1.0	1.0	0.1	97.9	10	6.1
234.4	1.5	3.0	0.5	95.0	3	10.8
278.0	0.1	0.1	1.5	98.3	22	5.5
367.0	2.0	0.1	0.1	97.8	17	8.7
400.8	0.1	0.1	1.5	98.3	31	6.6
409.0	0.1	0.1	0.5	99.3	13	7.0
425.2	0.5	0.1	0.0	99.4	9	7.9
466.3	3.5	2.5	1.0	94.0	19	7.0
514.5	0.1	2.0	0.1	97.8	2	6.3
607.5	1.0	0.0	0.0	99.0	9	9.7
691.9	4.0	0.0	0.0	96.0	9	10.2
719.9	4.5	0.1	0.0	95.5	23	15.4
755.9	0.1	0.5	0.0	99.4	8	6.7
784.2	8.0	0.1	0.0	91.9	6	12.3
846.7	2.0	0.1	0.0	97.9	33	8.0
940.5	0.5	0.5	1.5	97.5	3	7.1
1036.3	0.1	0.1	0.0	99.8	<1	7.6
1247.5	1.0	0.1	0.5	98.4	<1	6.9
1466.7	0.0	0.5	0.1	99.4	<1	6.0
1550.5	0.1	0.1	0.0	99.8	12	7.5
1672.3	0.0	0.0	0.1	99.9	6	7.5

Table 3
XRF major element analyses of the freshest SOH 1 lavas. $Fe_2O_3^*$ is total iron. All values in wt.%. A.I. = Alteration Index: 1—unaltered; 2—thin iddingsite rims on olivine; 3—extensive iddingsite alteration of olivine, 4—matrix altered and vesicles have secondary mineral linings; 5—high temperature minerals present (e.g. talc). LOI-loss on ignition. Analysts: T. Hulsebosch

Depth (m)	SiO_2	TiO_2	Al_2O_3	$Fe_2O_3^*$	MnO	MgO	CaO	Na_2O	K_2O	P_2O_5	LOI	SUM	A.I.
14.0	50.52	2.92	13.51	12.98	0.17	6.64	10.09	2.46	0.55	0.32	0.00	100.15	1.5
36.3	49.47	2.30	12.69	12.91	0.17	9.78	10.36	1.93	0.45	0.26	0.00	100.32	1.5
57.3	49.21	2.35	12.50	12.90	0.16	10.07	10.62	1.93	0.43	0.24	0.00	100.41	1
67.1	50.52	3.51	13.37	13.94	0.18	5.52	9.41	2.68	0.69	0.38	0.00	100.16	1
109.1	51.00	3.54	13.64	13.39	0.17	5.32	9.23	2.77	0.73	0.43	0.15	100.21	1
125.0	49.52	2.50	13.23	11.95	0.16	7.98	11.67	2.06	0.53	0.27	0.00	99.86	1.5
147.5[a]	50.24	3.01	13.83	13.04	0.17	6.35	10.31	2.45	0.57	0.33	0.00	100.28	1.5
165.5	50.27	2.85	13.85	13.39	0.17	6.12	10.28	2.25	0.56	0.30	0.00	100.04	1
176.8	50.64	2.83	13.72	12.78	0.17	6.10	10.02	2.41	0.61	0.34	0.00	99.61	1
192.0	50.24	2.97	13.22	13.40	0.17	7.06	9.82	2.33	0.54	0.31	0.19	100.04	1
211.5	50.21	2.46	13.54	12.72	0.17	7.28	10.74	2.01	0.40	0.23	0.00	99.77	2
234.4[a]	49.58	2.04	12.62	11.87	0.16	10.80	10.58	1.91	0.36	0.20	0.00	100.11	1
263.6	50.81	2.64	13.95	12.71	0.17	6.45	10.41	2.22	0.52	0.27	0.00	100.14	1
278.0	50.49	3.41	13.32	14.01	0.18	5.50	9.52	2.59	0.64	0.37	0.00	100.02	1.5
300.2	50.84	3.17	13.49	13.82	0.17	5.52	9.52	2.49	0.69	0.37	0.00	100.08	1
319.4	50.32	2.57	13.52	12.66	0.17	7.04	10.81	2.16	0.41	0.26	0.00	99.89	1.5
334.1	50.09	2.22	13.29	12.52	0.16	8.14	10.41	1.98	0.37	0.21	0.09	99.40	1.5
353.0[a]	50.39	2.41	13.52	12.67	0.17	7.14	10.82	1.98	0.42	0.24	0.09	99.73	1
367.0	50.14	2.59	12.82	12.48	0.17	8.69	10.04	2.27	0.45	0.27	0.97	99.91	1.5
383.4	50.80	2.42	13.78	12.55	0.16	6.94	10.88	2.07	0.41	0.24	0.00	100.25	1.5
400.8[a]	50.60	2.55	13.84	12.48	0.17	6.62	10.64	2.10	0.42	0.24	0.00	99.65	1.5
409.0[a]	50.51	2.47	13.62	12.58	0.17	6.98	10.71	2.29	0.37	0.25	0.33	99.93	1.5
425.2	50.56	2.36	13.29	12.46	0.16	7.91	10.63	1.99	0.39	0.25	0.00	100.00	1.5
439.8	50.43	2.74	13.73	12.92	0.16	6.88	10.45	2.17	0.45	0.28	0.27	100.20	1
452.3	50.13	2.41	13.00	12.33	0.16	8.91	10.27	2.21	0.39	0.25	0.78	100.03	1
466.3	50.90	2.37	13.77	12.41	0.17	6.96	10.74	2.03	0.40	0.24	0.00	99.98	1
485.5[a]	50.86	2.71	14.12	12.60	0.16	6.50	10.68	2.26	0.53	0.29	0.13	100.70	1
499.3[a]	51.14	2.75	13.79	12.13	0.16	6.78	10.36	2.41	0.53	0.29	0.68	100.33	1
514.5	50.52	2.83	13.73	13.15	0.17	6.33	10.33	2.23	0.48	0.27	0.34	100.02	1
517.6	49.88	2.20	13.05	11.84	0.16	9.74	11.12	1.64	0.31	0.20	0.20	100.34	1
537.4[a]	50.88	2.46	13.87	11.91	0.16	7.44	10.46	2.23	0.48	0.29	0.00	100.16	1
562.8	50.65	2.31	13.49	12.32	0.16	7.28	11.17	2.02	0.42	0.24	0.27	100.04	1.5
589.8	50.50	2.19	13.45	12.57	0.16	7.86	11.01	1.99	0.40	0.24	0.03	100.36	1
624.8[a]	51.14	2.55	14.00	12.25	0.16	6.68	10.49	2.00	0.45	0.25	0.25	100.24	1
653.8[b]	50.75	2.84	13.78	12.86	0.16	6.69	10.29	2.19	0.57	0.31	0.00	100.41	1
663.9	49.69	2.50	12.81	12.28	0.17	9.34	10.40	2.16	0.47	0.25	0.02	100.04	1.5
670.9[a]	50.16	2.49	12.72	12.36	0.17	9.69	10.29	1.75	0.43	0.24	0.00	100.27	1.5
684.3	50.25	2.57	13.61	12.39	0.17	7.27	10.88	2.20	0.41	0.26	0.00	99.98	2
691.9[a]	49.77	2.69	12.51	12.82	0.17	10.23	9.61	1.85	0.50	0.27	0.00	100.39	1.5
707.7	50.23	2.72	12.66	12.20	0.16	8.80	10.92	1.85	0.54	0.28	0.00	100.35	2
717.5	50.66	2.83	12.97	12.86	0.18	7.30	10.09	2.38	0.45	0.29	0.43	100.00	1.5
719.9	48.52	1.95	10.64	13.33	0.17	15.40	8.41	1.55	0.26	0.20	2.22	100.41	1.5
722.4	50.77	2.44	13.44	12.31	0.17	7.48	10.48	2.26	0.44	0.24	0.16	100.01	1.5
740.4	51.05	2.36	13.50	11.99	0.16	7.28	10.65	2.26	0.39	0.23	0.00	99.83	–
755.9[a]	50.97	2.57	13.97	12.53	0.17	6.72	10.67	2.02	0.44	0.26	0.00	100.29	2
805.3	49.99	2.21	13.08	11.87	0.16	9.76	11.14	1.64	0.31	0.20	0.20	100.34	1
806.5	50.70	2.25	13.41	12.25	0.16	8.25	10.48	1.87	0.39	0.18	0.00	99.94	1
825.4	50.24	2.22	13.11	12.19	0.17	8.92	9.93	1.74	0.39	0.19	0.99	100.08	1.5
846.7[b]	50.11	2.40	13.55	12.11	0.17	7.96	10.94	2.27	0.35	0.26	0.92	100.10	2
881.2	49.27	2.27	12.93	12.06	0.17	9.10	10.25	2.11	0.40	0.23	1.10	99.88	–
910.3	49.84	2.23	13.05	12.30	0.17	8.91	10.44	2.08	0.35	0.23	0.34	99.94	–

Table 3 (*continued*)

Depth (m)	SiO_2	TiO_2	Al_2O_3	$Fe_2O_3^*$	MnO	MgO	CaO	Na_2O	K_2O	P_2O_5	LOI	SUM	A.I.
940.5[a,c]	50.51	2.51	13.79	12.50	0.16	7.14	10.63	2.08	0.34	0.23	–	99.89	2
983.0[c]	50.39	2.09	12.77	11.99	0.16	9.69	11.52	1.77	0.34	0.19	–	99.11	3
991.8[b]	49.00	2.48	13.50	12.44	0.15	6.63	9.71	1.92	0.41	0.24	1.83	98.32	2.5
1036.3[b]	50.33	2.48	13.27	12.51	0.17	7.60	10.57	2.17	0.34	0.26	0.44	100.14	2.5
1098.3[b]	49.00	2.45	12.32	12.25	0.17	9.78	10.16	2.03	0.33	0.25	1.17	99.90	3
1217.7[b]	49.97	2.85	13.31	12.67	0.17	7.04	10.17	2.33	0.40	0.29	0.79	100.00	3
1247.5[b]	50.09	2.68	13.40	12.65	0.16	6.90	10.21	2.33	0.40	0.29	1.17	100.27	3
1291.1[b]	49.83	2.63	13.35	12.59	0.16	6.78	10.13	2.32	0.39	0.29	1.43	99.89	2.5
1466.7[b]	49.55	2.89	13.34	12.71	0.16	5.96	9.70	2.51	0.62	0.33	2.03	99.78	2.5
1550.5[a]	48.07	2.63	13.12	11.78	0.15	7.52	10.72	2.21	0.36	0.28	3.21	100.06	3.5
1672.3[c]	50.29	2.54	13.32	12.90	0.17	7.53	10.25	2.54	0.46	0.36	–	100.34	4.5

[a] Sample for geochronology.
[b] Dike sample.
[c] S. Quane.

flows; 16 are from dikes. Most of the lava flows and all of the dikes are weakly to moderately olivine phyric with no, or only minor amounts of clinopyroxene and plagioclase phenocrysts (Table 2). Plagioclase and clinopyroxene phenocrysts commonly show resorption and/or complex zoning, which are indicative of magma mixing in Hawaiian tholeiitic lavas (e.g. Garcia, 1996). Spinel and glass inclusions are common in olivine from SOH 1 lavas. The groundmass of these lavas consists of plagioclase and clinopyroxene with lesser amounts of olivine, ilmenite, magnetite, and glass. The vesicularity of the flow units ranges widely (1–33 vol.%, averaging ~12 vol.%; Table 2). The vesicularity of dikes range from 0 to 15 vol.% but most have <1 vol.%.

Twelve hyaloclastite samples and one carbonate breccia were also petrographically examined. The hyaloclastites are aphyric to sparsely olivine, plagioclase, and clinopyroxene phyric. They contain varying proportions of angular to sub-rounded glassy shards ranging in size from <1 to 10 mm in diameter. Most shards are thinly coated with alteration minerals (clay, calcite, and aragonite) and some of the hyaloclastites have calcite partially filling matrix voids.

There is no systematic variation in mineralogy with depth in the core except an increase in alteration minerals. The intensity of rock alteration was classified based on thin section analysis. An alteration index, ranging from 1 to 5, was assigned to each of the samples (see Table 3 for explanation of values). The subaerial rocks show little to no alteration except clay along fractures; the alteration index for these rocks ranges from 1 to 2.5 (except the more altered samples at 692, 720, and 722 m). The intensity of alteration increases markedly below the submarine–subaerial boundary with the most altered samples at the base of the hole (Fig. 3). The alteration mineralogy of the submarine rocks grades with depth from smectite, pyrite, and aragonite near the subaerial–submarine boundary to cristobalite, chalcedony, calcite, zeolite, and talc at the bottom of the hole (Bargar et al., 1995). For more information on the hydrothermal mineralogy of SOH 1 rocks, see Bargar et al. (1995).

5. Whole rock geochemistry

The same eighty samples examined in thin section were analyzed for major and trace elements by X-ray fluorescence spectrometry (XRF) at the University of Hawaii using a Siemens 303AS XRF spectrometer (Table 3). Samples were ground in a tungsten carbide grinding mill for less than 2 min to minimize contamination by the grinding vessel. Loss-on-ignition (LOI) was determined by weight loss after 8 h of heating at 900°C. The XRF sample procedures of Norrish and Hutton (1969) and Chappel (1991) were used. For major elements, two fused buttons were made for each sample using a lithium tetraborate flux. A powder pellet was pressed for trace element analysis, which was analyzed in duplicate.

Alteration is always a concern when dealing with

Table 4
XRF determined trace element abundances for the freshest SOH 1 samples (analyst; T. Hulsebosch)

Depth (m)	Nb	Zr	Y	Sr	Ni	Cr	V	Co	Zn	Cu
14.0	17.6	199	32.8	343	100	213	338	71	120	130
36.3	13.7	167	27.8	346	227	490	291	59	105	102
57.3	14.0	156	27.2	331	256	524	283	58	105	103
67.1	21.2	240	38.4	377	70	51	356	59	124	132
109.1	24.4	275	41.8	373	72	51	385	59	153	126
125.0	18.7	174	27.2	398	150	392	316	50	101	100
147.5	19.3	211	33.4	390	81	118	318	52	117	126
165.5	17.2	194	33.1	377	67	76	318	45	113	128
176.8	19.0	220	37.2	366	83	140	326	45	121	117
192.0	17.7	196	31.9	340	151	160	364	67	124	99
211.5	11.9	152	28.7	321	110	278	304	51	109	103
234.4	11.7	125	22.5	293	300	624	269	77	100	123
263.6	15.7	186	32.0	343	84	158	336	47	113	99
278.0	20.7	236	38.1	359	63	38	396	68	136	93
300.2	20.8	242	39.1	384	64	34	354	43	122	117
319.4	14.1	163	28.5	322	86	245	314	64	110	105
334.1	13.4	142	26.4	293	143	383	297	62	103	140
353.0	14.9	155	28.2	315	80	263	332	61	107	99
367.0	14.1	165	27.8	315	210	502	298	62	108	112
383.4	14.7	157	27.7	335	82	201	280	50	101	115
400.8	15.1	160	28.2	316	87	170	333	68	169	63
409.0	13.0	155	27.2	320	71	221	289	57	103	108
425.2	15.2	160	27.0	325	135	347	315	60	109	111
439.8	18.5	183	30.2	350	112	195	332	55	111	104
452.3	14.0	154	26.4	307	212	534	302	61	105	86
466.3	14.9	155	28.0	313	88	212	326	60	108	95
485.5	18.6	186	29.8	368	88	130	323	54	111	103
499.3	15.9	182	30.1	337	109	207	318	50	112	98
514.5	16.7	174	30.4	336	75	99	310	50	110	128
517.6	13.0	131	23.1	306	212	585	273	60	95	107
537.4	17.8	186	31.0	338	141	289	314	52	102	73
562.8	15.9	160	27.3	329	104	284	309	53	107	137
589.8	16.1	156	26.3	341	131	361	284	58	102	97
624.8	15.2	180	31.1	347	98	183	320	58	119	106
653.8[a]	17.9	195	30.7	365	116	193	328	55	114	128
663.9	14.2	150	25.4	305	230	462	300	115	100	64
670.9	22.0	155	26.6	327	238	463	273	75	103	56
684.3	15.0	158	27.2	326	114	258	311	78	106	68
691.9	16.8	175	27.5	344	325	425	281	58	113	47
707.7	17.3	179	27.2	370	184	501	291	57	104	93
717.5	16.0	185	31.8	323	151	289	325	67	109	142
719.9	11.0	124	21.8	269	538	861	216	74	104	85
722.4	13.9	159	27.3	304	122	294	318	74	112	131
740.4	12.6	152	27.0	301	108	334	312	62	113	131
747.1	10.3	103	17.5	598	119	326	216	41	69	159
755.9	17.5	161	28.3	340	86	241	275	54	98	131
805.3	12.9	139	24.4	283	184	501	292	77	107	108
806.5	13.2	150	27.7	305	143	424	314	56	109	118
825.4	13.1	146	27.3	292	175	474	313	66	109	121
846.7[a]	13.7	147	25.4	300	142	436	301	76	147	111
881.2	13.5	142	24.1	312	182	503	311	64	120	110
910.3	14.0	146	24.9	293	198	536	306	76	107	115
991.8[a]	14.6	173	30.7	335	99	161	327	51	117	132

Table 4 (*continued*)

Depth (m)	Nb	Zr	Y	Sr	Ni	Cr	V	Co	Zn	Cu
1036.3[a]	13.8	161	26.9	314	114	310	319	68	109	124
1098.3[a]	15.5	159	25.2	319	276	606	309	72	111	105
1217.7[a]	16.9	187	29.5	334	134	262	334	65	116	117
1247.5[a]	17.3	187	29.8	336	128	254	335	52	115	115
1291.1[a]	17.3	189	30.0	337	120	230	343	55	116	115
1466.7[a]	19.2	205	34.0	336	76	57	380	59	113	130
1550.5	18.5	173	27.4	382	146	318	339	50	103	135

[a] Sample is a dike.

rocks in a hydrothermally active area like the KERZ. Two geochemical parameters were used to evaluate the extent of alteration in the SOH 1 drill core: LOI and K_2O/P_2O_5 ratio. The LOI results show that the subaerial SOH 1 lavas experienced little or no alteration (>90% have LOI values <0.35 wt.%; Fig. 3), which is consistent with the thin section petrography results (Table 2). In contrast, there is a marked increase in alteration in the submarine section with LOI values up to 13.5 wt% just below the subaerial/submarine transition, although LOI values range widely in the submarine section (0.3–20.7 wt%; Fig. 3). The K_2O/P_2O_5 ratio of Hawaiian tholeiitic basalts is commonly used to evaluate their extent of weathering because K is leached during near surface alteration and P is not (e.g. Frey et al., 1994). The SOH 1 subaerial lavas have a restricted range in K_2O/P_2O_5 (1.4–2.0; Fig. 3), which is typical of Kilauea magmatic values (e.g. Wright, 1971). In contrast, rocks from the submarine section (lavas, hyaloclastites, and dikes) have a wide range in K_2O/P_2O_5 with both higher and lower values (0.6–9.3; Fig. 3). The samples with ratios >2 have relatively high K_2O contents and generally higher LOI values (up to 20.7 wt%) but there is no correlation of LOI, rock type, or vesicularity with K_2O/P_2O_5. For the evaluation of Kilauea's magmatic history, samples with LOI > 2.25%, K_2O/P_2O_5 <1.3 or >2.2, and alteration indices >2.5 were excluded, except for the two freshest samples from the lower part of the hole. These deleted samples represent ~30% of the 80 analyzed SOH 1 samples and are all from the submarine section.

All of the SOH 1 lavas are shield-building tholeiites based on the Macdonald and Katsura (1964) classification. For Hawaiian tholeiites, MgO is the most useful major element for evaluating compositional variation because olivine is the most common phenocryst. MgO contents in SOH 1 lavas range from 5.3 to 15.4 wt.%, with the majority of values between 6 and 10 wt.% (Table 3). A similar range was reported for Hilina basalts (6–18 wt.% MgO; Chen et al., 1996). There is no systematic variation of MgO with depth in SOH 1 (Fig. 4) but there is a general correlation between decreasing MgO content and increasing TiO_2, K_2O, Al_2O_3 (Fig. 4), SiO_2, Fe_2O_3, and P_2O_5. The wide range in major element concentrations at any given MgO wt.%, is indicative of a range of compositionally distinct parent magmas for SOH 1 lavas. Al_2O_3 and CaO contents decrease below 6.8 wt.% MgO, which is the distinction for differentiated Kilauea lavas (Wright 1971). These trends are indicative of plagioclase and clinopyroxene fractionation, which is consistent with both phases being phenocrysts in evolved SOH 1 rocks (Table 2). The increase in Al_2O_3/CaO ratio with decreasing MgO suggests that clinopyroxene is the dominant fractionating phase in these differentiated rocks (Fig. 4). Among the 20 analyzed a'a lavas, 17 are differentiated. Differentiated lavas are uncommon elsewhere on Kilauea and their abundance among the lavas in the lower east rift zone is an indication of the infrequent supply of magma to this part of the volcano (e.g. Wright, 1971).

Among the trace elements (Table 4), Nb, Zr, Sr, V and Y behave incompatibly. Plots of these elements vs. K define linear trends with considerable scatter compared to analytical error (Fig. 5), which is probably related to multiple parental magmas. Ni and Cr are strongly compatible elements in SOH 1 lavas.

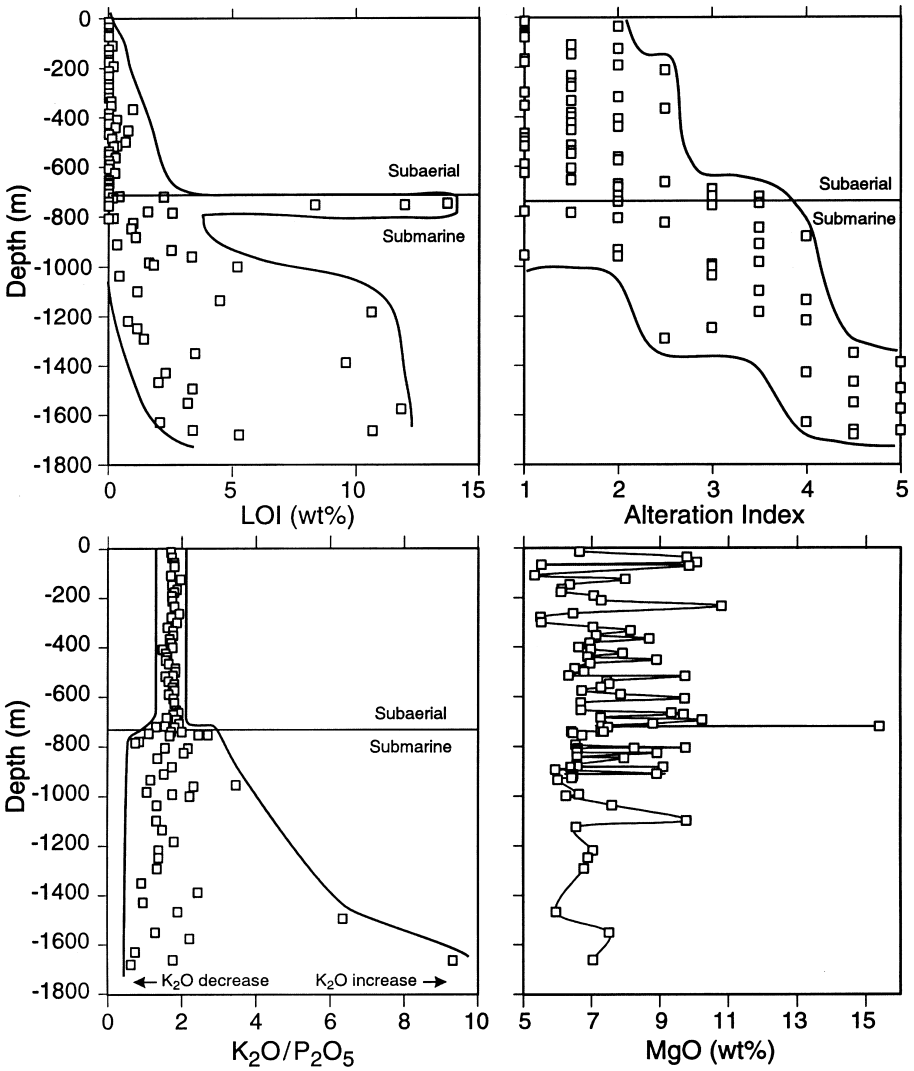

Fig. 3. Plots of alteration index, loss-on-ignition (LOI), MgO and K_2O/P_2O_5 vs. depth for SOH 1 lavas. Alteration index is based petrographic examination of 80 thin sections (see Table 3 for details). Loss on ignition is wt.% loss after 8 h of heating at 900°C. The alteration index and LOI values increase markedly at the submarine–subaerial transition, as does the range in K_2O/P_2O_5. The MgO plot only includes rocks meeting the alteration criteria (LOI $< 2.25\%$, $K_2O/P_2O_5 > 1.3$ and <2.2, and alteration indices <2.5). There is no systematic variation of MgO with depth and most of the SOH 1 lavas contain 6–10 wt.% MgO.

When plotted against an incompatible element, these elements define trends with negative slopes and considerable scatter (Fig. 5), which may be the result of both magma mixing and crystal fractionation from multiple parent magmas. None of the trace elements show systematic variations with depth in the section (Fig. 5) nor is there a systematic change in trace element ratios with depth (Fig. 6).

6. Glass geochemistry

Glass compositions were measured at the University of Hawaii using a Cameca SX-50, five-spectrometer electron microprobe. Natural glass and mineral standards including VG2, A99, OR-1-5, Apatite and Troilite were used for this study. A PAP-ZAF correction was applied to all analyses and minor corrections

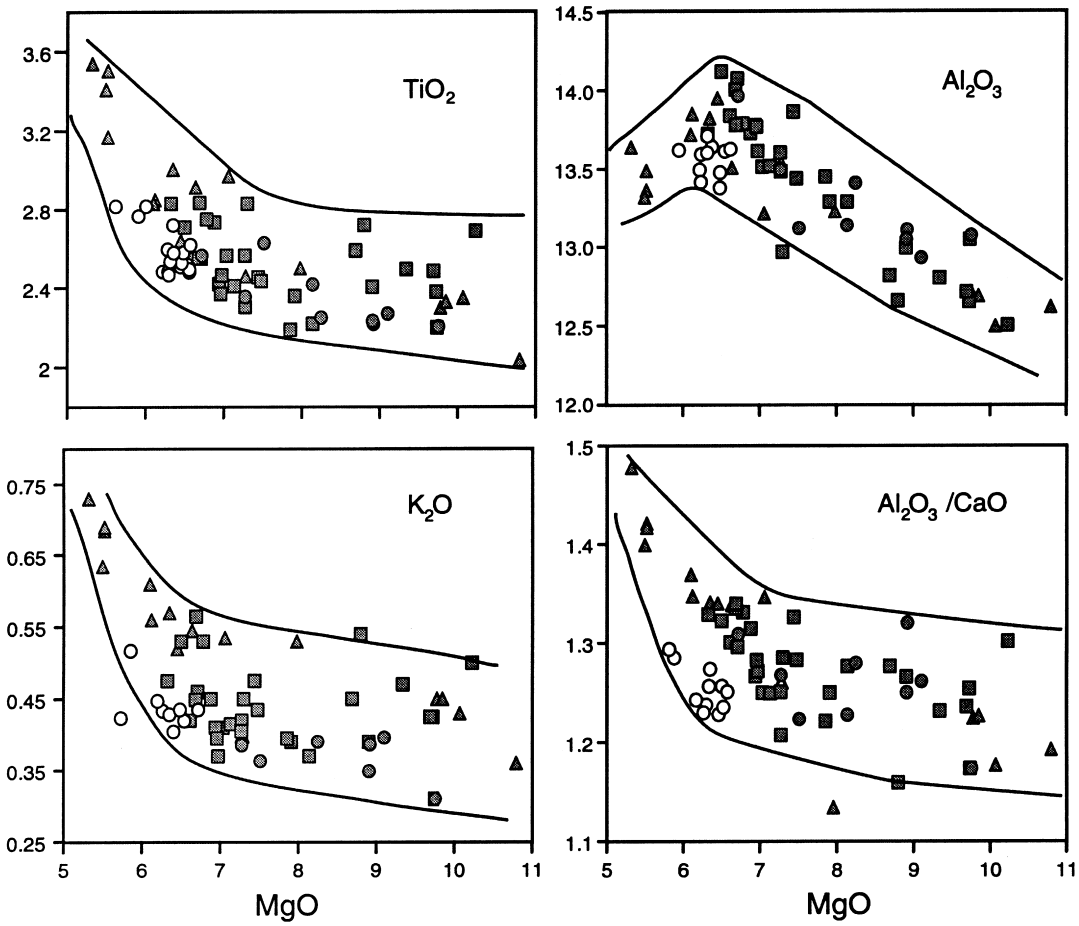

Fig. 4. MgO variation diagrams for SOH 1 lavas meeting alteration criteria (see Fig. 3 caption). Triangles represent samples recovered from <300 m depth, squares 300–722 m depth, and circles >722 m depth (open circles are for glasses from >722 m; Table 5). All oxides are in wt.%. The kink in the variation trends at 6.5–7.0 wt.% MgO marks the transition from olivine-only basalts to differentiated lavas. Error bars are smaller than symbols.

(<2%) were made, based on repeated analysis of Smithsonian glass standards A99 and VG2, to obtain the final values. A 10 nA, defocused beam (spot size ~10 μm) was used. Peak counting times of 70 s for Fe, Mg, Ti, and Si, 40 s for Ca, Na, and K, and 100 s for S, Al, and P were used with background counting times half of the peak times. The reported analyses are averages of five spot analyses per sample.

Glasses from 18 hyaloclastites were microprobed (Table 5) to determine compositional variation in the submarine section of the core where few massive basalts are available for whole rock analyses (740–1123 m). S analyses are useful for qualitatively determining the depth of eruption of the glasses (e.g. Moore and Clague, 1992). Quenching temperatures for Kilauea glasses can be estimated using Helz and Thornber (1987) geothermometer. The glasses have a very limited range in MgO content (5.9–6.6 wt.%, with 85% between 6.4 and 6.6 wt.%), CaO content (10.3–11.2 wt.%) and K_2O (0.39–0.52) indicating that they were derived from similar parental magmas and were quenched at similar temperatures (1135–1145°C). These glasses have the same compositional range as the submarine lavas (i.e. relatively low K_2O compared to the younger subaerial lavas; Fig. 4). The S contents of these hyaloclastite glasses are low (0.01–0.07 wt.%, with all but three <0.04 wt.%). The lower values are thought to be indicative of

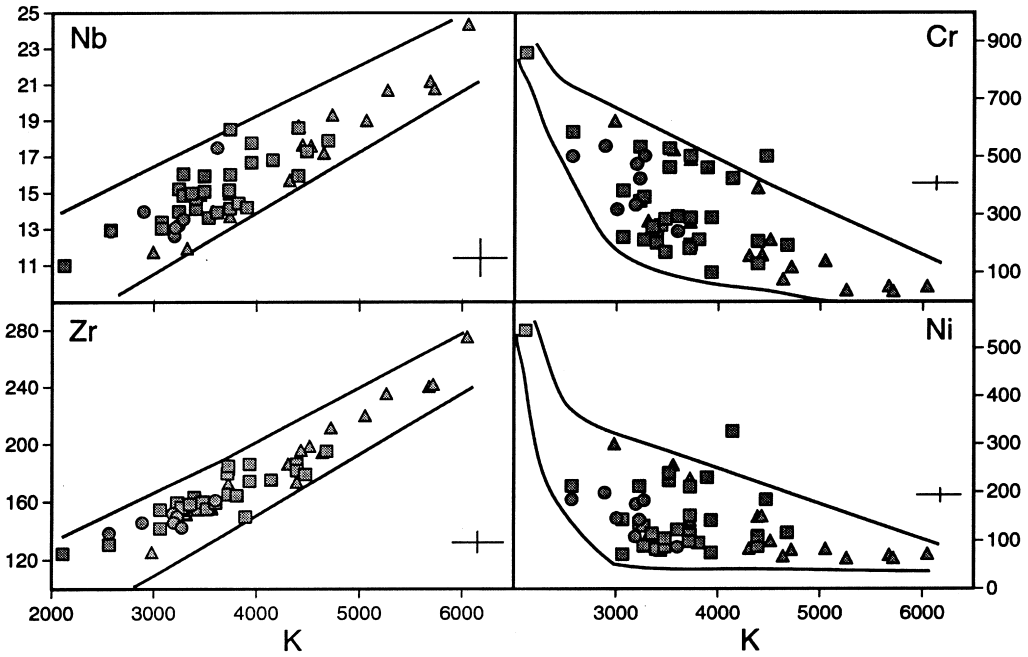

Fig. 5. K variation diagrams for Nb, Zr, Cr, and Ni for SOH 1 lavas meeting alteration criteria. All values are in ppm and symbols are the same as in Fig. 4. The incompatible elements form linear trends with scatter well beyond analytical error. The scatter for the compatible elements (Cr and Ni) may be related to magma mixing; the scatter in the Nb and Zr data require distinct parental magmas. Two sigma error bars are given in lower right corner for each plot.

Table 5
Electron microprobe glass analyses of hyaloclastites from SOH 1 (analyses are in wt%; total iron as Fe_2O_3; analysts; S. Quane and M. Garcia)

Depth (m)	SiO_2	TiO_2	Al_2O_3	Fe_2O_3	MgO	CaO	Na_2O	K_2O	P_2O_5	S	Total
740	51.48	2.47	13.43	11.79	6.35	10.73	2.34	0.40	0.18	0.02	99.16
746	51.58	2.47	13.52	11.80	6.39	10.80	2.32	0.38	0.17	0.01	99.43
793	51.16	2.53	13.52	11.81	6.47	11.02	2.27	0.42	0.20	0.02	99.40
808	50.97	2.47	13.55	11.76	6.53	10.99	2.32	0.42	0.19	0.02	99.19
814	51.04	2.51	13.56	11.82	6.52	11.04	2.29	0.42	0.20	0.00	99.40
824	51.16	2.53	13.56	11.86	6.51	11.00	2.30	0.41	0.18	0.02	99.51
841	51.07	2.54	13.54	11.83	6.52	11.01	2.25	0.42	0.21	0.02	99.38
870	51.09	2.55	13.53	11.77	6.50	11.03	2.27	0.42	0.20	0.02	99.35
880	51.16	2.59	13.46	12.06	6.52	10.85	2.31	0.43	0.20	0.03	99.57
883	51.08	2.49	13.55	11.87	6.33	10.96	2.30	0.43	0.21	0.02	99.21
888	51.03	2.60	13.48	12.05	6.32	10.93	2.31	0.43	0.22	0.02	99.37
893	50.89	2.81	13.15	12.84	5.88	10.19	2.34	0.44	0.22	0.07	98.76
911	51.08	2.59	13.57	11.98	6.40	10.95	2.28	0.43	0.21	0.02	99.49
919	51.00	2.56	13.53	11.97	6.39	11.05	2.30	0.42	0.20	0.02	99.42
927	50.23	2.73	13.67	12.14	6.36	10.73	2.24	0.44	0.21	0.06	98.73
934	50.52	2.77	13.57	12.34	5.95	10.53	2.38	0.52	0.22	0.04	98.80
998	51.05	2.81	13.21	12.42	6.18	10.64	2.34	0.45	0.22	0.01	99.33
1123	51.03	2.62	13.42	12.01	6.49	10.98	2.27	0.42	0.22	0.02	99.45

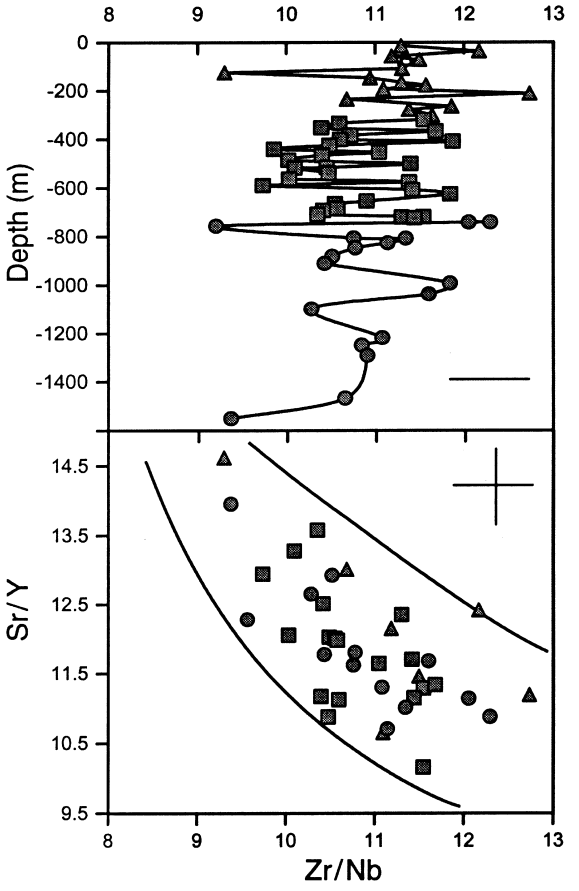

Fig. 6. Zr/Nb vs. depth and Sr/Y for SOH 1 lavas meeting alteration criteria. Only lavas with MgO > 7 wt.% are used for Sr/Y plot to avoid the affects of plagioclase fractionation on Sr. There is no systematic variation for these immobile trace element ratios with depth. There is a wide range in composition for each depth range, as observed for historical Kilauea lavas (Pietruszka and Garcia, 1999). Two sigma error bars are shown in lower right (depth plot) and upper right (Sr/Y plot) corners.

subaerial eruption; the higher values are indicative of shallow submarine (<500 m) eruption (see Moore and Clague, 1992; Garcia, 1993).

7. Temporal geochemical variation of Kilauea

When we began this study of rock cores from a 1.7 km deep drill hole, we anticipated finding lavas from either the preshield stage of Kilauea and/or from neighboring Mauna Loa Volcano. To our surprise, neither was encountered. The SOH 1 core contains no rocks with preshield stage compositions (i.e. lower SiO_2, higher $Na_2O + K_2O$ tholeiites, transitional, or alkalic lavas, which typify Loihi Volcano, the type example of preshield stage Hawaiian volcanism; e.g. Moore et al., 1982). Also, there is no indication of a change in geochemistry with depth towards pre-shield stage compositions. Furthermore, all of the SOH 1 lavas have Kilauea-like compositions, which are distinct from those of neighboring Mauna Loa Volcano. For example, SOH 1 lavas have relatively high concentrations of the immobile incompatible elements Ti and Nb, a characteristic difference between the lavas from the two volcanoes (Fig. 7). It should be noted that there are a few unpublished analyses of Mauna Loa submarine southwest rift lavas (J.M. Rhodes, 1998, pers. comm.) with Kilauea-like major and trace element compositions but they are interbedded with and subordinate (~10%) to lavas having typical Mauna Loa compositions (Fig. 8). Although some Mauna Loa rocks with Kilauea-like compositions could be present in the SOH 1 core, it is unlikely due to the absence of any lavas with Mauna Loa-like compositions within the core.

Overall, the SOH 1 rocks are similar in major element chemistry to both the oldest exposed Kilauea surface lavas, the prehistoric Hilina basalts, and to the youngest Kilauea lavas from the ongoing Puu Oo eruption (Chen et al., 1996; Garcia et al., 1996). The only trend noted for major element variation with depth for the SOH 1 lavas is that the submarine rocks have lower K_2O than the upper subaerial rocks (<300 m; Fig. 4), although the intermediate depth rocks overlap both groups with no depth trend. Hilina Basalts have lost K due to weathering (Chen et al., 1996), so we cannot compare their K variation with the SOH 1 results. No other long-term systematic geochemical variation is apparent for the SOH 1 section (Figs. 4–5), which is consistent with the lack of a temporal compositional variation for the Hilina Basalts (Chen et al., 1996). Compared to the Hilina Basalts and historical Kilauea summit lavas (<210 years; Pietruszka and Garcia, 1999), SOH 1 lavas display only slightly more trace element and less major element variation (Fig. 8), despite the much greater age range represented by the SOH 1 samples.

Recent studies of Hawaiian volcanoes (e.g. Frey

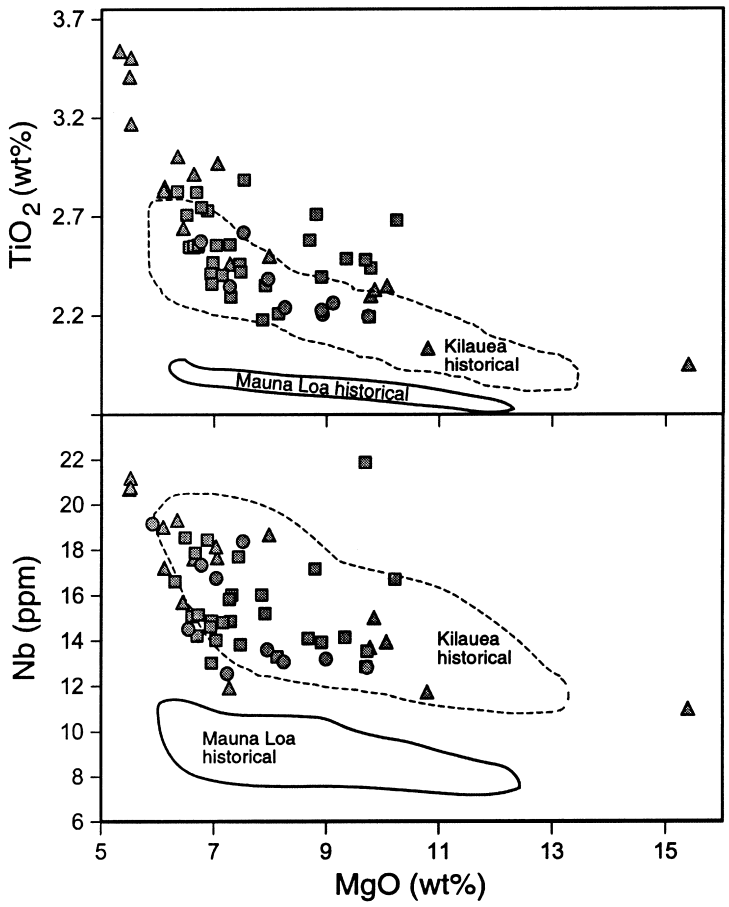

Fig. 7. MgO variation diagrams for Nb and TiO_2 in SOH 1 lavas meeting alteration criteria. Nb and TiO_2 define distinct fields for historical Mauna Loa (<160 years old, field bounded by solid line; Rhodes and Hart, 1995) and Kilauea summit lavas (field bounded by dashed line; Pietruszka and Garcia, 1999; Garcia unpub. data). The SOH 1 lavas plot well above the Mauna Loa field and mostly within the narrow field for Kilauea historical lavas (<210 years old). Symbols as in Fig. 4; errors are about the size of the symbols.

and Rhodes, 1993; Frey et al., 1994; Roden et al., 1994; Kurz et al., 1995; Rhodes and Hart, 1995; Chen et al., 1996) have shown that Sr and Pb isotopes are well correlated with incompatible trace element ratios involving Nb. Thus, these trace element ratios reflect different source components for Hawaiian lavas (Rhodes, 1996). Rhodes et al. (1989) also found that TiO_2/Al_2O_3, which is sensitive to partial melting variations, distinguishes Kilauea from Mauna Loa lavas. SOH 1 lavas have Kilauea-like Zr/Nb and TiO_2/Al_2O_3 (Fig. 8). Hence, Kilauea's source and melting conditions may have remained essentially the same over the last 350 ka.

8. Age of Kilauea Volcano

Kilauea Volcano is one of the world's most active volcanoes and is presently in its shield-building stage. This stage is thought to be comprised entirely of tholeiitic rocks and to last 500 ka (Moore and Clague, 1992) to 900 ka (Guillou et al., 1997a). Little was known prior to the SOH drilling program study about how long Kilauea had been in the shield building stage because of the rapid resurfacing rate of Kilauea (Holcomb, 1987) and the absence of geochronological ages >23 ka (Easton, 1987). The unspiked K–Ar dates and rock chemistry from SOH 1 (Tables 1 and 3) show that Kilauea has erupted shield stage

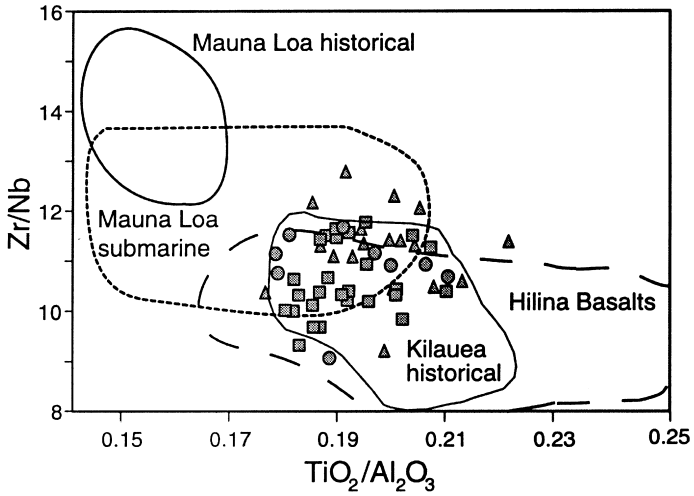

Fig. 8. TiO_2/Al_2O_3 vs. Zr/Nb plot for SOH 1 lavas (symbols as in Fig. 4), Kilauea summit historical lavas (field bounded by solid line; Garcia unpublished), Hilina Basalts (long dashed lines; Chen et al., 1996), Mauna Loa submarine lavas (field bounded by dashed line; Rhodes unpub. data), and Mauna Loa historical lavas (field bounded by solid line; Rhodes and Hart, 1995). Rhodes et al. (1989) demonstrated that this plot was effected in discriminating historical lavas of Mauna Loa from those of Kilauea. The SOH 1 data plot mostly within the field for historical Kilauea lavas but partially overlap with the rare older submarine Mauna Loa lavas with Kilauea-like compositions.

tholeiites for at least ~350 ka. This relatively old age is consistent with the 436 ± 47 ka age for a tholeiitic lava from SOH 4 (Guillou et al., 1997b) from a somewhat greater depth. There is geochemical evidence that the old SOH 4 lava is from a section of rocks with Mauna Loa compositions (i.e. higher $^{87}Sr/^{86}Sr$ and Zr/Nb ratios and lower $^{206}Pb/^{204}Pb$ ratios than typical Kilauea rocks; H. West, 1998 unpublished data). However, the presence of rocks with Kilauea-like geochemistry ~210 m above the dated sample suggests that Kilauea lavas in SOH 4 are probably ~400 ka.

If Kilauea had a pre-shield stage, which is believed to occur in all Hawaiian volcanoes (Walker, 1990), and the duration of this stage was similar to Loihi's (~250 ka; Guillou et al., 1997a), then Kilauea's age may be ~600–650 ka. This age is markedly greater than previous estimates for the age of Kilauea based on magma supply rates and surface exposures (e.g. 150 ka, Lipman, 1995; 200–300 ka, Easton, 1978). It is, however, in agreement with the ~600 ka age predicted for Kilauea based on lava accumulation rates from the Hawaiian Scientific Drilling Project pilot hole (DePaolo and Stolper, 1996). Their volcano growth model also predicts that Kilauea is ~60% of the way through its shield building stage (DePaolo and Stolper, 1996). If this estimate is correct, and Kilauea follows the general evolutionary model for Hawaiian shield volcanoes with a pre-shield (~250 ka for Loihi; Guillou et al., 1997a) and a post-shield (~240 ka for Mauna Kea; Frey et al., 1990), the entire life span for Kilauea would be ~1150 ka. This estimate is consistent with recent estimates for the life span of Hawaiian volcanoes (~1000 ka, Lipman, 1995; ~1400 ka, Guillou et al., 1997a).

9. Lava accumulation rates for Kilauea's east rift zone

Lava accumulation rates for Kilauea's east rift zone can be estimated using the new K–Ar ages for SOH 1. The oldest sample gives an overall growth rate of ~4.4 mm/year. If the other ages are considered individually, the rate increases upsection (5.4, 27 and 81 mm/year). Similar but less dramatic increases in growth rate are evident for the nearby SOH 4 drill hole (3.8–11 mm/year; Guillou et al., 1997b). Combining the ages from these two holes, which are only ~8 km apart, a trend of progressively increasing lava accumulation emerges (curved trend in Fig. 9).

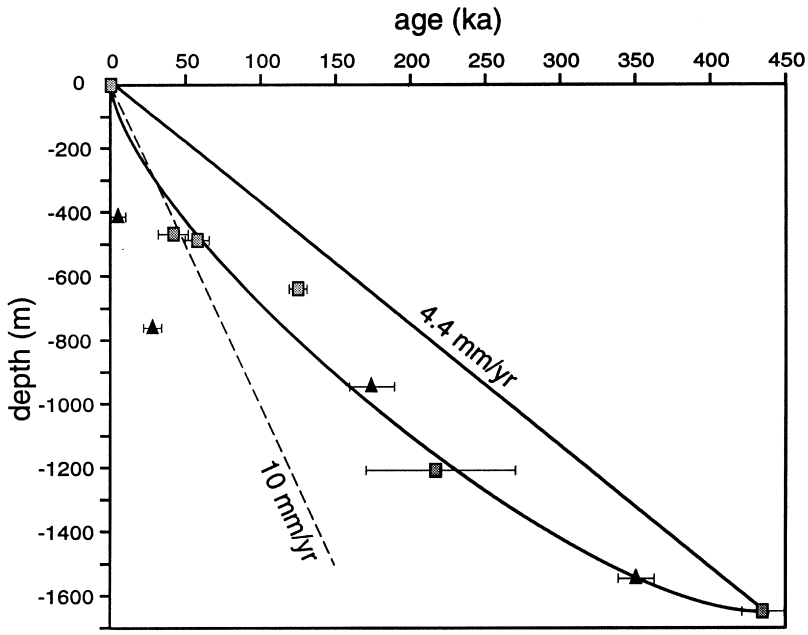

Fig. 9. Lava accumulation rates for Kilauea's lower east rift zone based on ages from SOH 1 (triangles) and SOH 4 (squares) lavas. The 4.4 mm/year line is a linear accumulation rate based only on the oldest dated SOH lava and ignores the presence of dikes (most abundant below 1200 m in SOH 1 and below 1000 m in SOH 4). If the ages from two drill holes are combined, a pattern of increasing lava accumulation rate emerges even if the older lavas are ignored (because of the presence of dikes of unknown but younger age). The lavas from above the intense dike zones in these two holes to 500 m may have accumulated at ~4 mm/year but the younger lavas seem to have accumulated more rapidly (~10 mm/year). The two younger SOH 1 lavas have ages that seem too young for their position in the section.

This trend is somewhat muted by the contribution to the deeper section of these holes (>1200 m for SOH 1 and >1000 m for SOH 4) from dikes. If the dikes in these two holes are removed, the lava accumulation rate trend upsection increases more dramatically from rates of 1–2 mm/year near the base to ~10 mm/year for the upper section of the holes.

A lava accumulation rate of 10 mm/year for upper SOH lavas is somewhat higher than any previously calculated rate for the flanks of Hawaiian volcanoes (e.g. 7.8 ± 3.2 mm/year for Mauna Kea; Sharp et al., 1996; 4.3 mm/year Mauna Loa; Lipman and Moore, 1996) but much lower than the rates estimated for the summits of Hawaiian volcanoes (25–35 mm/year; DePaolo and Stolper, 1996). The relatively high lava accumulation rate determined here for the east rift zone may be indicative of the dominance of this rift zone over Kilauea's other rift zone (>90% of historically erupted rift zone lavas; Macdonald et al., 1983). Likewise, the cause for the increase in lava accumulation rate in the SOH sections is probably related to the development of east rift zone as a major locus of Kilauea's volcanism rather than to an increase in its magma supply rate (see below).

10. Long-term magma supply rates for Kilauea

Determining the magma supply rate for any volcano is inherently problematic. For example, estimates for Kilauea's magma supply rate based on summit tiltmeter and leveling surveys utilize simplistic point source models for inflation of its summit reservoir and ignore passive movement of magma into rift zones (e.g. Dzurisin et al., 1984). For periods prior to tiltmeters and leveling surveys, eruption volumes are used to infer magma supply rates. Periods of sustained eruptions, such as the current eruption of Kilauea, are thought to give more reliable estimates (e.g. Dvorak and Dzurisin 1993), although they must also be considered minimum rates because of

endogenous growth of the volcano (e.g. Francis et al., 1993). These methods indicate wide variations in the magma supply rate (0.01–0.12 km^3/year; Pietruszka and Garcia, 1999) for Kilauea's historical period (1790–1998).

To avoid many of the problems in estimating Kilauea's historical magma supply rate, we have taken published volume estimates for the volcano ($15–22.5 \times 10^3$ km^3; Bargar and Jackson, 1974; Lipman 1995; DePaolo and Stolper, 1996) and our estimated age for Kilauea shield volcanism (~400 ka) to calculate a 'long-term' magma supply rate. A correction for Kilauea's preshield stage is not needed because it would be minor compared to the difference in the volume estimates for the volcano (10%, assuming a volume similar to Loihi's preshield stage, 0.75×10^3 km^3; Garcia et al., 1995). Dividing the volume estimates by the age yields a long-term magma supply rate of 0.05 ± 0.01 km^3/year for Kilauea. This value is remarkably similar to the estimated average historical rate of 0.06 km^3/year (Dvorak and Dzurisin, 1993). If magma compositions are primarily controlled by the extent of partial melting (e.g. Watson and McKenzie, 1991), then the narrow range of Kilauea lava compositions for the last 350 ka supports the interpretation that the volcano's overall magma supply rate probably has remained relatively constant during this period.

11. Implications for the structure of the Hawaiian plume

Hawaii has played a central role in understanding mantle plumes because so much is known about its volcanoes and underlying plate compared to other plumes. For example, Hawaiian volcanoes show a systematic compositional variation during the later stages of shield (e.g. Mauna Loa; Kurz et al., 1995) and post-shield volcanism (e.g. Haleakala; Chen et al., 1991), which is thought to be related to compositional heterogeneity in the Hawaiian plume (e.g. Lassiter et al., 1996). The age of the Pacific plate under Hawaii is ~105 Ma (Waggoner, 1993) and recent estimates have it moving towards the northwest at ~12 cm/year (Wessel and Kroneke, 1997). It is assumed that the Hawaiian plume is stationary compared to the motion of the Pacific plate. These observations and assumptions have been used to infer a radially zoned structure for the Hawaiian plume with a ~100 km wide melt extraction zone (Watson and McKenzie, 1991; DePaolo and Stolper, 1996) and a ~50 km wide central core that feeds shield-stage volcanism (e.g. Lassiter et al., 1996). Previous studies have suggested that Kilauea is located on the margin of this central core (e.g. Lassiter et al., 1996; Hauri et al., 1996). The geochronological and geochemical results for SOH 1 lavas allow us to evaluate these models for the structure and size of the Hawaiian plume.

If the plume remains stationary relative to the Pacific plate, the oldest reliable age for SOH 1 lavas (351 ka) and the velocity of Pacific plate motion for Hawaii (12 cm/year; Wessel and Kroneke, 1997) indicate that Kilauea Volcano may have sampled a 42 km long section of the Hawaiian plume (or 48 km, if Kilauea's shield stage volcanism has been active for 400 ka). During this period, the composition of Kilauea magmas remained remarkably consistent based on SOH 1 lava compositions (Tables 3 and 4). Therefore, the portion of the plume supplying Kilauea must be well mixed (i.e. shows no sign of the large-scale heterogeneity that characterizes later stages of Hawaiian volcano growth; Chen et al., 1991) and continually changing to allow a "fresh" portion of the plume to be melted. Neighboring Mauna Loa Volcano, which erupts geochemically distinct lavas (Fig. 7), is only ~35 km from Kilauea. Thus, the area of the plume that has been melted to form Kilauea is <35 km wide (perhaps ~30 km) and ~48 km long, or ~1130 km^2. If the volume of Kilauea is ~20,000 km^3 and its lavas are produced by 5–10% melting (Watson and McKenzie, 1991; Pietruszka and Garcia, 1999), then ~150,000 km^3 of the plume was melted to form Kilauea. Therefore, a ~130 km thick region of the plume would have been melted to form Kilauea, which is considerably thicker than previous estimates of the melting thickness in the Hawaiian plume (~55 km; Watson and McKenzie, 1991; ~70 km; Ribe and Christensen, 1999). Either these models underestimated the thickness of the zone of melting within the plume, or the core of the plume is not stationary.

Kilauea is estimated to be ~60% of the way through its shield-building stage (DePaolo and Stolper, 1996). Therefore, the plume core diameter may

be 70–80 km where Kilauea passes over it. This interpretation assumes that the mantle magma conduit is not deformed during the life of the volcano. Unfortunately, there are too few earthquakes under Mauna Loa, which is near the end of its shield stage (Moore and Clague, 1992), to allow the orientation of its deep mantle conduit to be determined (Klein et al., 1987). If Kilauea has preshield and postshield stages of similar duration to those of adjacent volcanoes (~250 ka each), then a ~140 km-wide zone of melt extraction might be needed for Kilauea. This estimate is larger than previous estimates of ~100 km for the width of the primary melt extraction region of the Hawaiian plume but is smaller than a new estimate of ~180 km based on a dynamic model for plume melting (Ribe and Christensen, 1999).

12. Conclusions

The lavas from the ~1.7 km deep SOH 1 drill hole are virtually identical in mineralogy and composition to historical Kilauea lavas. The new geochronological data for SOH 1 confirm previous dating of drill core from another Kilauea east rift zone drill hole (SOH 4; Guillou et al. 1997b) demonstrating that Kilauea has been producing shield-building stage tholeiitic lavas for at least 350 ka, probably 400 ka. If Kilauea had a preshield stage of similar duration to Loihi Volcano (~250 ka; Guillou et al. 1997a), its overall age would be at least 600 ka, which is much older than previous field-based studies but consistent with a theoretical model for its age (DePaolo and Stolper, 1996). Our estimate of the average long-term (~350 ka) magma supply rate for Kilauea's shield building is nearly identical to a recent estimate for Kilauea's historical magma supply rate (0.05 ± 0.01 vs. $0.06\ km^3$/year; Dvorak and Dzurisin, 1993). The overall consistency in the geochemistry of SOH 1 lavas and of Kilauea's magma supply rate suggests neither the melting conditions nor the source for Kilauea lavas has changed significantly during the past 350 ka.

The age and geochemistry of the SOH lavas can be used to infer the size of the Hawaiian plume based on a few observations and assumptions. If the Pacific plate has been moving 12 cm/year for the last few million years (Wessel and Kroneke, 1997) and the plume is stationary relative to the motion of the Pacific plate, SOH 1 lavas sampled ~42 km of the core of the Hawaiian plume (48 km, if the 400 ka age is used). During its shield stage, the composition of Kilauea magmas remained remarkably consistent based on SOH 1 lava compositions (Tables 3 and 4). Therefore, the portion of the plume supplying Kilauea must be well mixed (i.e. shows no sign of the large-scale heterogeneity that characterizes later stages of Hawaiian volcano growth; Chen et al., 1991) and continually changing to allow a "fresh" portion of the plume to be melted. Thus, the simplistic cartoons for the structure of the Hawaiian plume which place Kilauea near the edge of a radially zoned plume (e.g. Lassiter et al., 1996) need modification to accommodate a well-mixed source for at least the last 350 ka.

If the plume remains stationary relative to the Pacific plate, then the portion of the Hawaiian plume that has been melted to form Kilauea is about 48 km long, 30 km wide and 130 km deep, which is much greater than previous estimates. Although the location of the plume may be stationary, the mass within the plume may move faster than the Pacific plate and replenish the region that is producing Kilauea magmas.

Acknowledgements

We are grateful to Laurent Turpin for providing the opportunity for SQ to do geochronology work at the Laboratoire des Sciences du Climat et de l'Environnement (CEA-CNRS), to Nathalie Max for the precise K analyses, and Jean Francois Tannau for technical support with the geochronology work, Frank Trusdell, Aaron Pietruszka, and Nathan Becker for insightful discussions about Kilauea, to G. Fitton, A.D. Johnston, Don Thomas and Scott Rowland for reviews on this paper, and to H. West and J.M. Rhodes for use of their unpublished geochemical data. This work was supported by a Geological Society of America graduate student research grant, the University of Hawaii Harold Stearns and William Coulbourn fellowships (all to S. Quane), and by the National Science Foundation for support of the Hawaii Scientific Drilling Project (EAR-9528534; D. Thomas, P.I.) and Kilauea research (EAR-9614247; M. Garcia, P.I.). This is SOEST contribution no. 5204.

References

Bargar, K.E., Jackson, E.D., 1974. Calculated volumes of individual shield volcanoes along the Hawaiian-Emperor Chain. U.S. Geol. Surv. J. Res. 2, 762–766.

Bargar, K.E., Keith, Terry, E.C., Trusdell, F.A., 1995. Fluid inclusion evidence for past temperature fluctuations in the Kilauea east rift zone geothermal area, Hawaii. Geothermics 24, 639–659.

Cassignol, C., Gillot, P.Y., 1982. Range and effectiveness of unspiked potassium–argon dating. In: Odin, G.S. (Ed.), Numerical Dating in Stratigraphy. Wiley, New York, pp. 159–179.

Chappel, B.W., 1991. Trace element analysis of rocks by X-ray spectrometry. Adv. X-ray Anal. 34, 263–276.

Chen, C.Y., Frey, F.A., Garcia, M.O., Dalrymple, G.B., Hart, S., 1991. Geochemistry of the tholeiitic to alkalic basalt transition, Haleakala Volcano, Hawaii. Contrib. Mineral. Petrol. 106, 183–200.

Chen, C.Y., Frey, F.A., Rhodes, J.M., Easton, R.M., 1996. Temporal geochemical evolution of Kilauea Volcano: comparison of Hilina and Puna Basalt. In: Basu, A., Hart, S.R. (Eds.). Earth Processes: Reading the Isotopic Code. Am. Geophys. Monogr., 95, 161–181.

DePaolo, D.J., Stolper, E.M., 1996. Models of Hawaiian volcano growth and plume structure: implications of results from the Hawaii Scientific Drilling Project. J. Geophys. Res. 101, 11,643–11,654.

Dvorak, J.J., Dzurisin, D., 1993. Variations in magma supply at Kilauea Volcano, Hawaii. J. Geophys. Res. 98, 22,255–22,268.

Dzurisin, D., Koyanagi, R.Y., English, T.T., 1984. Magma supply and storage at Kilauea Volcano, Hawaii, 1956–1983. J. Volcanol. Geotherm. Res. 21, 177–206.

Easton, R.M., 1978. Stratigraphy and petrology of the Hilina formation: the oldest exposed lavas of Kilauea Volcano. MS Thesis, Univ. Hawaii at Manoa, Honolulu, Hawaii, 274 pp.

Easton, R.M., 1987. Stratigraphy of Kilauea Volcano. In: Decker, R.W., Wright, T.L., Stauffer, P.H. (Eds.). Volcanism in Hawaii. U.S. Geol. Surv. Prof. Paper, 1350, 243–260.

Francis, P., Oppenheimer, C., Stevenson, D., 1993. Endogenous growth of persistently active volcanoes. Nature 366, 554–557.

Frey, F.A., Rhodes, J.M., 1993. Intershield geochemical differences among Hawaiian volcanoes: implications for source compositions, melting process and magma ascent paths. Philos. Trans. R. Soc. London A 342, 121–136.

Frey, F.A., Wise, W.S., Garcia, M.O., West, H., Kwon, S.T., Kennedy, A., 1990. Evolution of Mauna Kea Volcano, Hawaii: Petrologic and geochemical constraints on postshield volcanism. J. Geophys. Res. 95, 1271–1300.

Frey, F.A., Garcia, M.O., Roden, M.F., 1994. Geochemical characteristics of Koolau Volcano: implications for of intershield geochemical differences among Hawaiian volcanoes. Geochim. Cosmochim. Acta 58, 1441–1462.

Garcia, M.O., 1993. Pliocene–Pleistocene volcanic sands from site 842: products from giant landslides. Proc. Ocean Drilling Program, Sci. Res. 136, 53–63.

Garcia, M.O., 1996. Petrography and olivine and glass chemistry of lavas from the Hawaii Scientific Drilling Project. J. Geophys. Res. 101, 11,701–11,713.

Garcia, M.O., Foss, D.J.P., West, H.B., Mahoney, J.J., 1995. Geochemical and isotopic evolution of Loihi Volcano, Hawaii. J. Petrol. 36, 1647–1674.

Garcia, M.O., Rhodes, J.M., Trusdell, F.A., Pietruszka, A.J., 1996. Petrology of lavas from the Puu Oo eruption of Kilauea Volcano: III. The Kupaianaha episode (1986–1992). Bull. Volcanol. 58, 359–379.

Gillot, P.Y., Cornette, Y., 1986. The Cassignol technique for K–Ar dating, precision and accuracy: examples from the Pleistocene to recent volcanics from southern Italy. Chem. Geol. 59, 205–222.

Guillou, H., Garcia, M.O., Turpin, L., 1997. Unspiked K–Ar dating of young volcanic rocks from Loihi and Pitcairn hotspot seamounts. J. Volcanol. Geotherm. Res. 78, 239–249.

Guillou, H., Turpin, L., Garnier, F., Charbit, S., Thomas, D.M., 1997. Unspiked K–Ar dating of Pleistocene tholeiitic basalts from the deep core SOH-4, Kilauea, Hawaii. Chem. Geol. 140, 81–88.

Hauri, E.H., Lassiter, J.C., DePaolo, D.J., 1996. Osmium isotope systematics of drilled lavas from Mauna Loa, Hawaii. J. Geophys. Res. 101, 11,793–11,806.

Helz, R., Thornber, C., 1987. Geothermometry of Kilauea Iki lava lake, Hawaii. Bull. Volcanol. 49, 651–668.

Holcomb, R.T., 1987. Eruptive history and long-term behavior of Kilauea volcano. In: Decker, R.W., Wright, T.L., Stauffer, P.H. (Eds.). Volcanism in Hawaii. U.S. Geol. Surv. Prof. Pap. 1350, 261–350.

Klein, F.W., Koyanagi, R.Y., Nakata, J.S., Tanigawa, W.R., 1987. The seismicity of Kilauea's magma system. U.S. Geol. Surv. Prof. Pap. 1350, 1019–1185.

Kurz, M.D., Kenna, T.C., Kammer, D.P., Rhodes, J.M., Garcia, M.O., 1995. Isotopic evolution of Mauna Loa Volcano: a view from the submarine southwest rift. In: Rhodes, J.M., Lockwood, J.P. (Eds.), Mauna Loa Revealed: Structure, Composition, History, and Hazards. Am. Geophys. Union, Monogr. 92, 289–306.

Lassiter, J.C., DePaolo, D.J., Tatsumoto, M., 1996. Isotopic evolution of Mauna Kea Volcano: results from the Hawaiian Scientific Drilling Project. J. Geophys. Res. 101, 11,769–11,780.

Lipman, P.W., 1995. Growth of Mauna Loa during the last hundred thousand years, rates of lava accumulation versus gravitational subsidence. In: Rhodes, J.M., Lockwood, J.P. (Eds.), Mauna Loa Revealed: Structure, Composition, History, and Hazards. Am. Geophys. Union Monogr. 92, 45–80.

Lipman, P.W., Moore, J.G., 1996. Mauna Loa lava accumulation rates at the Hilo drill site: formation of lava deltas during a period of declining overall volcanic growth. J. Geophys. Res. 101, 11,631–11,641.

Macdonald, G.A., Katsura, T., 1964. Chemical composition of Hawaiian lavas. J. Petrol. 5, 82–133.

Macdonald, G.A., Abbott, A.T., Peterson, F.L., 1983. Volcanoes in the Sea. Univ. Hawaii Press, Honolulu, 517 pp.

Moore, R.G., 1983. Distribution of differentiated tholeiitic basalts on the lower east rift zone of Kilauea Volcano, Hawaii: a possible guide for geothermal exploration. Geology 11, 136–140.

Moore, J.G., Clague, D.A., 1992. Volcano growth and evolution of the island of Hawaii. Geol. Soc. Am. Bull. 104, 1471–1484.

Moore, J.G., Clague, D.A., Normark, W.R., 1982. Diverse basalt types from Loihi Seamount, Hawaii. Geology 10, 88–92.

Norrish, K., Hutton, J.T., 1969. An accurate X-ray spectrographic methods for the analysis of a wide range of geochemical samples. Geochim. Cosmochim. Acta 33, 431–441.

Pietruszka, A.J., Garcia, M.O., 1999. A rapid fluctuation in the source and melting history of Kilauea Volcano inferred from the geochemistry of its historical summit lavas (1790–1982). J. Petrol. 40, 1321–1342.

Rhodes, J.M., 1996. Geochemical stratigraphy of lava flows samples by the Hawaii Scientific Drilling Project. J. Geophys. Res. 101, 11,729–11,746.

Rhodes, J.M., Hart, S.R., 1995. Episodic trace element and isotopic variations in historical Mauna Loa lavas: implications for magma and plume dynamics. In: Rhodes, J.M., Lockwood, J.P. (Eds.), Mauna Loa Revealed: Structure, Composition, History, and Hazards. Am. Geophys. Union Monogr. 92, 263–288.

Rhodes, J.M., Wenz, K.P., Neal, C.A., Sparks, J.W., Lockwood, J.P., 1989. Geochemical evidence for invasion of Kilauea's plumbing system by Mauna Loa magma. Nature 337, 257–260.

Ribe, N.M., Christensen, U.R., 1999. The dynamic origin of Hawaiian volcanism. Earth Planet. Sci. Lett. 171, 517–531.

Roden, M.F., Trull, T., Hart, S.R., Frey, F.A., 1994. New He, Sr, Nd, and Pb isotopic constraints on the constitution of the Hawaiian Plume: results from Koolau Volcano, Oahu, Hawaii. Geochim. Cosmochim. Acta 58, 1431–1440.

Sharp, W.D., Turrin, B.D., Renne, P.R., Lanphere, M.A., 1996. The $^{40}Ar/^{39}Ar$ and K/Ar dating of lavas from the Hilo 1-km core hole, Hawaii Scientific Drilling Project. J. Geophys. Res. 101, 11,607–11,616.

Sleep, N.H., 1990. Hotspots and mantle plumes: some phenomenology. J. Geophys. Res. 95, 6715–6736.

Steiger, R.H., Jäger, E., 1977. Convention on the use of decay constants in geo- and cosmochronology. Earth Planet. Sci. Lett. 36, 359–362.

Tilling, R.I., Dvorak, J.J., 1993. Anatomy of a basaltic volcano. Nature 363, 125–133.

Waggoner, D.G., 1993. The age and alteration of central Pacific oceanic crust near Hawaii, Site 843. Proc. Ocean Drilling Prog., Sci. Res. 136, 119–132.

Walker, G.P.L., 1990. Geology and volcanology of the Hawaiian Islands. Pac. Sci. 44, 315–347.

Watson, S., McKenzie, D., 1991. Melt generation by plumes: a study of the Hawaiian plume. J. Petrol. 32, 501–537.

Wessel, P., Kroenke, L.W., 1997. A geometric technique for relocating hotspots and refining absolute plate motions. Nature 387, 365–369.

Wright, T.L., 1971. Chemistry of Kilauea and Mauna Loa lava in space and time. U.S. Geol. Surv. Prof. Pap. 735, 40 pp.